Multicarrier Waveform Processing for HF Communications

Juha Yli-Kaakinen*, Juuso Alhava*, Markku Renfors*, and Hannu Tuomivaara†
*Laboratory of Electronics and Communications Engineering, Tampere University of Technology, Finland
{juha.yli-kaakinen, juuso.alhava, markku.renfors}@tut.fi
†Kyynel Ltd, Oulu, Finland
hannu.tuomivaara@kyynel.net

***Abstract*—High-frequency (HF) band communications can be flexibly realized using multicarrier modulation (MCM) techniques. HF channels are typically characterized by severe multipath effects and high Doppler spreads requiring advanced estimation and equalization methods as well as elaborate waveform design for addressing these issues. This paper compares the performance of three widely utilized MCM techniques, namely, cyclic prefix (CP) orthogonal frequency-division multiplexing (OFDM), filter bank multicarrier/offset-QAM (FBMC/OQAM), and filtered multitone (FMT) in HF communications. In addition, the filtered variant of CP-OFDM is included in the comparison. The performance of these systems is simulated using commonly adopted HF-channel models. Channel estimation is carried out using scattered pilots with minimum mean-squared error based interpolation schemes whereas the equalization is realized using frequency-sampling based subcarrier equalizer. It is shown that the simulated uncoded bit-error rate of CP-OFDM is superior when compared with FBMC/OQAM and FMT even in the case when CP-OFDM waveform is filtered for better spectral containment. In addition, the implementation complexity and peak-to-average power ratio performance of (filtered) CP-OFDM compare favourable with FBMC/OQAM and FMT.**

I. Introduction

High-frequency (HF) communication technology is widely employed for military, maritime, and aeronautical systems as well as world-wide broadcasting services [1]–[4]. It provides the most flexible and cost effective long-range infrastructure-independent wireless technology for organizations involved in emergency, crisis, remote, and military communications. On the other hand, long-distance communication over HF channels (3 to 30 MHz band) is known to be challenging due to rapidly changing propagation conditions and disturbances.

Single-carrier systems traditionally used for point-to-point HF communications require highly-complex equalizers to combat with doubly-dispersive (i.e., time and frequency selective) communication channels. Multicarrier modulation (MCM) schemes, in addition to their inherent flexibility, relieve the requirements of the equalizer by transmitting the data stream over the group of narrow-band (quasi) flat-fading subchannels. However, in the case of time variability, each subcarrier experiences Doppler spreading destroying the subcarrier orthogonality and, consequently, resulting to degradation of the performance. Therefore, also in the case MCM schemes, the waveform design plays an important role for achieving the best performance with respect to constraints dictated by the technology requirements, e.g., configurability, spectral efficiency, time-frequency localization, peak-to-average power ratio (PAPR), and latency.

In this paper, the performance of the three commonly adopted MCM techniques [5] are compared by simulating their performance with HF-channel models defined in digital radio mondiale (DRM) standard. These techniques are, namely, cyclic prefix (CP) orthogonal frequency-division multiplexing (OFDM), filter bank multicarrier/offset-QAM (FBMC/OQAM), and filtered multitone (FMT). In addition, a spectrally well localized variant of CP-OFDM, so-called filtered-CP-OFDM (F-CP-OFDM) is included in the comparison.

The performance of these systems is simulated in three cases. In the first case, the perfect channel knowledge is assumed. In the second case, the channel is assumed to be know at scattered pilot positions [6] and the interpolation in time-frequency lattice is carried out using minimum mean-squared error (MMSE)-based estimation methods [7]. In the last case, least-squares (LS) estimate at pilot positions is first derived based on the transceived pilots and then MMSE-based interpolation is used to evaluate the channel characteristics at data symbol positions.

It is shown that the performance of CP-OFDM is superior with respect to FBMC/OQAM and FMT in the case of doubly-dispersive channel models. In addition, the narrow transition-band filtering used for improving the spectral containment of CP-OFDM only slightly deteriorates the waveform performance. In [8], the authors carried out the similar study using linear interpolation for scattered pilot based channel estimation, basically, showing the performance of each MCM scheme unfeasible for the most challenging propagation conditions. However, based on the current study, reliable high-rate communication link can be established even in the case of most severe scenarios provided that the waveform parameters, pilot structures, and equalizer realizations are properly selected.

The outline of the paper is as follows. First, the considered MCM waveforms are shortly introduced in Section II. Then, Section III discusses the computational complexities and the spectral efficiencies of these schemes. In Section IV, com-

978-1-5386-4559-8/18/$31.00

monly adopted HF channel models are reviewed. The scattered pilots based channel estimation and frequency-sampling based equalizer are discussed in Section V. Section VI describes the waveform design, the frame and pilot structures as well as prototype filter design. The simulation results are presented in Section VII whereas in Section VIII the conclusions are drawn.

II. Waveform Alternatives

A. CP-OFDM

CP-OFDM is the most important MCM scheme and it is extensively employed in modern broadband radio access systems. CP-OFDM combines simple and robust channel equalization, high flexibility in allocating spectral resources to different users as well as simplicity of employing multiantenna schemes with the core functionality [9].

The main restriction of basic CP-OFDM is the limited spectral containment resulting to high sensitivity to interferences from asynchronous spectral components and undesirable out-of-band emissions leading to an adjacent channel leakage. The spectral containment of the basic CP-OFDM can be improved by straightforward windowing or filtering. However, narrow transition-band time-domain filtering increases both the computational complexity [10] and the time-dispersion introduced by the channel [11].

The frequency-domain filtering scheme based on fast-convolution (FC) processing, provides an effective way to realize subband-filtered CP-OFDM schemes, with significantly lower computational complexity and highly increased flexibility when compared to time-domain filtering approaches [12]. In this contribution, F-CP-OFDM waveform processing is transparent in the sense that FC based filtering is utilized only on the transmitter side while the receiver uses conventional CP-OFDM processing.

B. FBMC/OQAM

Alternative MCM techniques are provided by the filter bank based methods of waveform processing and channelization filtering [13]–[15]. One of the most studied filter bank based waveform is FBMC/OQAM (filter bank multicarrier/offset-QAM, also known as OFDM/OQAM) [14], [15]. FBMC/OQAM has a considerably better time-frequency localization with respect to the basic CP-OFDM leading to a lower out-of-band emission and making it more robust to synchronization errors. The orthogonality of FBMC/OQAM is reached by using so-called offset-QAM modulation where the real and imaginary parts of the symbols are staggered at twice the Nyquist rate with the half symbol time offset [16]. The offset-QAM modulation introduces various challenges in developing effective pilot bases synchronization and estimation schemes and in applying certain multi-antenna configurations.

C. FMT

Another well-known filter bank scheme is FMT (also known as oversampled OFDM) [17]–[20]. FBMC/OQAM reaches maximal spectral efficiency by using significantly overlapping subcarriers, typically with the roll-off of one, whereas FMT uses non-overlapping subcarriers, and relatively small roll-off is chosen for reaching good spectral efficiency. The main benefit of FMT is that basic QAM modulation with Nyquist filtering can be used in subcarriers, which allows straightforward application of effective pilot based estimation and synchronization schemes. Also the multi-antenna configurations developed for CP-OFDM can be directly exploited.

TABLE I
Spectral efficiency of considered MCM schemes

MCM	Spectral efficiency
CP-OFDM [21]	$(T_s - T_{CP})/T_s < 1$
FBMC/OQAM [22]	$T_s\Delta_f = 1$
FMT [17]	$1/(1+\alpha) < 1$

III. Waveform Comparison

A. Spectral Efficiency

The spectral efficiency of CP-OFDM is limited by the required CP length and, correspondingly, the need for the non-overlapping subcarriers restricts the spectral efficiency of FMT. On the other hand, FBMC/OQAM can provide maximal spectral efficiency, by utilizing the real orthogonality instead of strict complex orthogonality. The spectral efficiencies of these MCM schemes are collected in Table I. Here, T_s and Δ_f denote the overall symbol duration and subcarrier spacing, respectively, whereas T_{CP} and α denote the CP duration and roll-off factor, respectively.

B. Implementation Complexity

The focus here is on the synthesis filter bank complexity, and the metric for the complexity is the number of real multiplications per transmitted complex symbol. Fast Fourier transform and inverse fast Fourier transform (IFFT) are the core modules in efficient realization of these waveforms and for a given transform length, FFT and IFFT have the same complexity. For power-of-two transform lengths, the split-radix algorithm is considered to be the most efficient one in terms of number of real multiplications [23] as given by

$$C(N) = N[\log_2(N) - 3] + 4, \tag{1}$$

where N is the transform length.

For basic CP-OFDM, only single IFFT block is required for the modulation and the number of real multiplications per complex symbol is thus given as

$$C_{\text{OFDM}}(M) = C(M)/M_{\text{act}}, \tag{2}$$

where M is IFFT size and M_{act} is the number of active subcarriers. In the case, when FC based processing is used for filtering the CP-OFDM waveform [12], then forward and inverse transforms of size M are required for each overlapping processing block as well as some complex-by-real multiplications resulting to following complexity:

$$C_{\text{F-CP-OFDM}}(M) = \left(C(M) + 2\Psi[C(M) + 2N_{\text{TB}}]\right)/M_{\text{act}}. \tag{3a}$$

TABLE II
PARAMETERS FOR THE HF CHANNEL MODELS D, E, AND F [4]

CHANNEL D	Path 1	Path 2		
Path delay (τ_k)	0.00 ms	2.00 ms		
Path gain, rms (ρ_k)	1.00	1.00		
Doppler shift (f_D)	0.00 Hz	0.00 Hz		
Doppler spread (B_D)	1.00 Hz	1.00 Hz		
CHANNEL E	Path 1	Path 2		
Path delay (τ_k)	0.00 ms	4.00 ms		
Path gain, rms (ρ_k)	1.00	1.00		
Doppler shift (f_D)	0.00 Hz	0.00 Hz		
Doppler spread (B_D)	2.00 Hz	2.00 Hz		
CHANNEL F	Path 1	Path 2	Path 3	Path 4
Path delay (τ_k)	0.00 ms	2.00 ms	4.00 ms	6.00 ms
Path gain, rms (ρ_k)	0.50	1.00	0.25	0.06
Doppler shift (f_D)	0.00 Hz	1.20 Hz	2.40 Hz	3.60 Hz
Doppler spread (B_D)	0.10 Hz	2.40 Hz	4.80 Hz	7.20 Hz

Here, N_{TB} is the number of transition-band weights and $\Psi \geq 1$ is given by

$$\Psi = (1 + M_{CP}/M)/(1 - \lambda), \tag{3b}$$

where M_{CP} is the CP length and the factor λ is determined by the ratio of the overlap between consecutive processing blocks and the processing block length.

The implementation for the FBMC/OQAM and FMT synthesis filter bank consist of a transform block and a polyphase filter of length KM, where the overlapping factor K is the ratio of the filter impulse response length to the multicarrier symbol period. Therefore, the complexity for these schemes can be expressed as

$$C_{FBMC/OQAM}(M) = C_{FMT}(M) = (C(M) + 2KM)/M_{act}, \tag{4}$$

assuming that the filter coefficients are real valued and staggering or two-times oversampling is carried out after the IFFT as described in [24].

IV. HF CHANNEL MODELS

Digital radio mondiale (DRM) is an universal, openly standardized digital broadcasting system defining six channel profiles to be considered for the low frequency (LF), medium frequency (MF), and HF [4]. These channel profiles employ Watterson-type channel model [25], [26]. This model is a linear time-variant model assuming that the received signal $s(t)$ is a linear combination of delayed versions of the input signal $\delta(t)$ as given by

$$s(t) = \sum_{k=1}^{N} \rho_k c_k(t) \delta(t - \tau_k). \tag{5}$$

Here, ρ_k is the gain of the path k, τ_k is the corresponding relative delay, and the time-variant tap weights $c_k(t)$ are zero-mean complex-valued stationary Gaussian random processes. The magnitudes $|c_k(t)|$ are Rayleigh distributed and the phases $\phi(t)$ are uniformly distributed. Each weight $c_k(t)$ is characterized by one stochastic process defined by its power spectral density (PSD) and variance. The PSD determines the average speed of variation in time and the relative gain ρ_k defines the variance of the signal, which is received through this path. The width of PSD is quantified by the Doppler spread B_D of that path whereas a non-zero center frequency of PSD is characterized by its Doppler shift (or Doppler frequency) f_D. The parameters for HF channel models D, E, and F used in this contribution are revised in Table II.

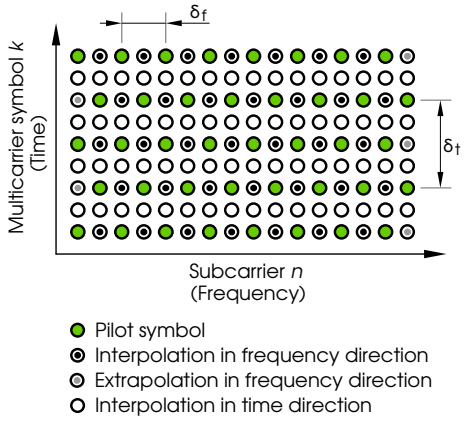

Fig. 1. Lattice-type pilot arrangement.

V. CHANNEL ESTIMATION AND EQUALIZATION

A. Scattered Pilot based Estimation

In the scattered pilot based methods, the overall channel estimate is obtained from the scattered channel estimates by two-dimensional (in time and frequency) interpolation. Fig. 1 depicts typical lattice-type pilot arrangement where pilot symbols are inserted periodically in the time-frequency lattice to serve as references for channel estimation. Let δ_t and δ_f denote the spacing of pilot symbols in time and frequency, respectively. In order estimate the characteristics of the frequency-selective and time-varying channel, the pilot-symbol arrangement has to satisfy [7]

$$\delta_t \leq \lceil 1/(2 f_{D_{max}} T_s) \rceil \quad \text{and} \quad \delta_f \leq \lceil 1/(2\tau_{max}\Delta_f) \rceil. \tag{6}$$

Here, T_s and $f_{D_{max}}$ denote the symbol duration and the maximum Doppler shift, respectively, whereas Δ_f and τ_{max} denote the subcarrier spacing and maximum delay spread, respectively.

The least-squares (LS) channel estimate at the pilot positions are obtained from transmitted and received pilot symbols $\mathbf{X}_p$ and $\mathbf{Y}_p$, respectively, as follows:

$$\widehat{\mathbf{H}}_{LS} = \left(\mathbf{X}_p^H \mathbf{X}_p\right)^{-1} \mathbf{X}_p^H \mathbf{Y}_p = \mathbf{X}_p^{-1} \mathbf{Y}_p. \tag{7}$$

The linear minimum mean-squared error (MMSE) estimate exploits the second-order statistics of the channel transfer function to minimize the mean-squared error (MSE). The MMSE estimate is given as [7]

$$\widehat{\mathbf{H}}_{MMSE} = \mathbf{R}_{\mathbf{H}} \left(\mathbf{R}_{\mathbf{H}} + \sigma_n^2 \mathbf{I}\right)^{-1} \widehat{\mathbf{H}}_{LS}, \tag{8}$$

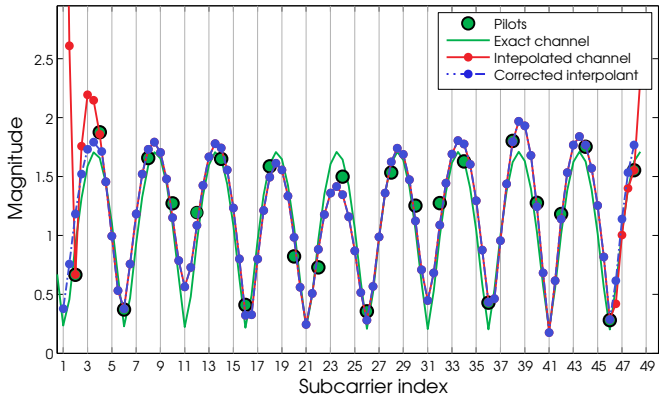

Fig. 2. MMSE channel estimate evaluated in frequency direction based on noisy pilots on HF channel model E.

where $\mathbf{R_H} = \mathbb{E}(\mathbf{H}\mathbf{H}^{\mathrm{H}})$ is the channel covariance matrix with $\mathbb{E}(\cdot)$ being expected value, σ_{n}^2 is the noise variance, and $\mathbf{I}$ is the identity matrix. The covariance matrix contains the correlations between the subcarriers at given time- and frequency spacing

$$\mathbb{E}(\mathbf{h}_{k,l}\mathbf{h}_{\bar{k},\bar{l}}^{\mathrm{H}}) = r_{\mathrm{t}}(k-\bar{k})r_{\mathrm{f}}(l-\bar{l}).$$

For a fading channel with Jakes' spectrum, the correlation in time direction $r_{\mathrm{t}}(\Delta_k)$ is expressed as

$$r_{\mathrm{t}}(\Delta_k) = \mathrm{J}_0(2\pi f_{\mathrm{D}_{\max}} T_{\mathrm{s}} \Delta_k), \tag{9}$$

where $\mathrm{J}_0(\cdot)$ is the Bessel function of first kind of order zero. Meanwhile, in an exponentially-decreasing multipath power delay profile, the correlation in the frequency direction is given as

$$r_{\mathrm{f}}(\Delta_l) = \frac{1}{1 + \mathrm{j}2\pi\tau_{\mathrm{rms}}\Delta_{\mathrm{f}}\Delta_l}, \tag{10}$$

where τ_{rms} is the root mean squared (RMS) delay spread.

The problem with the scattered pilots based estimation is, that at some edge subcarriers the estimation needs to be carried out using extrapolation due to the lack of pilots symbols (cf. Fig. 1). The extrapolation typically generates less accurate estimates and, therefore, result in a severe degradation of the performance. In this contribution, this problem has been solved by employing the correlation properties of the channel estimate by properly replicating the extrapolated parts of the channel estimates by the interpolated ones.

Fig. 2 illustrates the extreme case for HF channel model E, where the solid line with circle markers shows the oscillatory estimate at the edge subcarriers and the dot-dashed line with circle markers depicts the corrected estimate. It should be taken into account that the number of points to be interpolated between the pilots in frequency direction actually increases in the case of FMT and FBMC/OQAM due to the utilized multi-tap subcarrier-wise equalizers to be described later on. In this figure, three-tap equalizer is assumed requiring one additional interpolation point between the each pair of subcarriers.

The above estimator coefficients can evaluated off-line for a set of signal-to-noise ratio (SNR) values assuming that the expected maximum Doppler frequency and delay spread are known beforehand [27]. In this case, the real-time implementation requires only one matrix multiplication instead of matrix inversion and two matrix multiplications required for the general case.

B. Frequency-Sampling based Equalizer

In the case of CP-OFDM and F-CP-OFDM, as long as the channel delay spread and the possible synchronization errors remain within the CP time, the channel equalization can be straightforwardly carried out using subcarrier-wise multiplication by a complex coefficient value. This approach is also applicable for FBMC/OQAM and FMT, however, due to the not-so-good time localization of the filter bank waveforms, multi-tap frequency-sampling based subcarrier-wise equalizers with MSE criterion are typically used [6], [28].

The transfer function of a complex non-causal three-tap finite-impulse response (FIR) equalizer on subband m at time instant n can be expressed as

$$H_{\mathrm{EQ}}(z) = c_{m,n}^{(-1)} z + c_{m,n}^{(0)} + c_{m,n}^{(1)} z^{-1}, \tag{11}$$

where the filter coefficients $c_{m,n}^{(p)}$ for $p = \{-1, 0, 1\}$, are adjusted such that the frequency response of $H_{\mathrm{EQ}}(z)$ achieves at the desired frequency points the following target values:

$$\chi_{m,n}^{(p)} = \gamma \frac{\left(\widehat{H}_{m,n}^{(p)}\right)^*}{\left|\widehat{H}_{m,n}^{(p)}\right|^2 + \xi}. \tag{12}$$

Here, $p \in \{-1, 0, 1\}$, where $p = -1$ corresponds to the lower subband edge, $p = 0$ to the subband center, and $p = 1$ to the upper subband edge. $\widehat{H}_{m,n}^{(p)}$ is the estimated channel frequency response on subchannel m and time n at frequency position given by p whereas γ and ξ are scaling factors.

Now, the filter coefficients values can be determined from the target values as

$$c_{m,n}^{(-1)} = \frac{\chi_{m,n}^{(0)} z^{-2} - \chi_{m,n}^{(1)} z^{-1}(z^{-1}+1) + \chi_{m,n}^{(2)} z^{-1}}{1 - z^{-1} - z^{-2} + z^{-3}} \tag{13a}$$

$$c_{m,n}^{(0)} = \frac{-\chi_{m,n}^{(0)} z^{-1} + \chi_{m,n}^{(1)}(z^{-2}+1) - \chi_{m,n}^{(2)} z^{-1}}{(-1 + z^{-1})^2} \tag{13b}$$

$$c_{m,n}^{(1)} = \frac{\chi_{m,n}^{(0)} z^{-1} - \chi_{m,n}^{(1)} z^{-1}(z^{-1}+1) + \chi_{m,n}^{(-2)} z^{-2}}{1 - z^{-1} - z^{-2} + z^{-3}}, \tag{13c}$$

where $z = \exp(\mathrm{j}\omega_c)$ with $-\omega_c$ and ω_c, respectively, being the lower and upper subband edge frequencies.

Fig. 3 compares the bit error rate (BER) performance of FBMC/OQAM for one- three- and five-tap equalizers in HF channel model E with perfect channel knowledge. As seen from this figure, one-tap equalizer is clearly insufficient for this channel model whereas increasing the filter length to five only slightly improves the performance when compared with the three-tap equalizer.

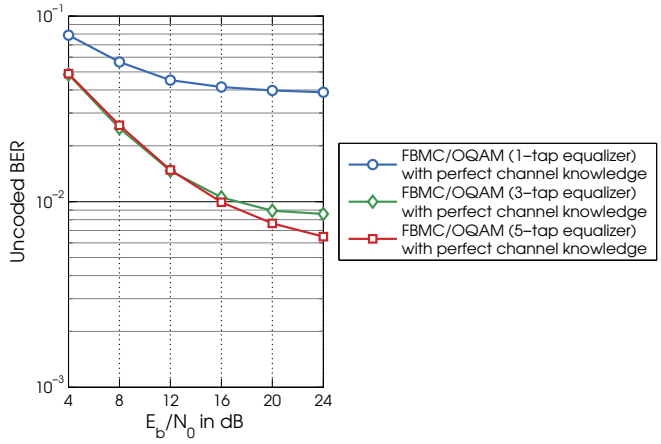

Fig. 3. Uncoded BER of FBMC/OQAM for one-, three- and five-tap equalizers in HF channel model E with perfect channel knowledge and QPSK modulation.

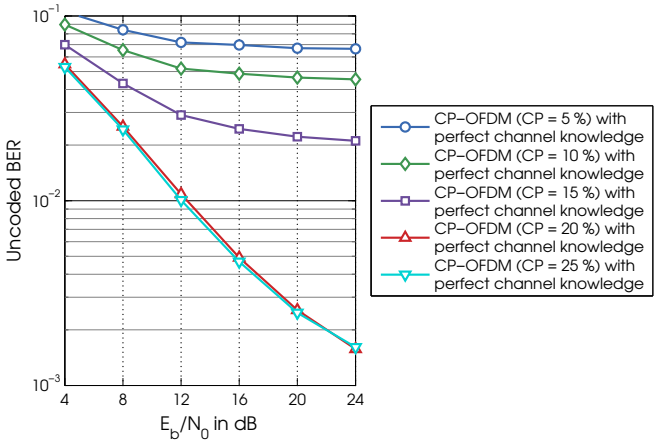

Fig. 4. Uncoded BER of basic CP-OFDM as a function of CP length in HF channel model E with perfect channel knowledge and QPSK modulation.

VI. Waveform Design

A. Subcarrier Spacing

In [8], the effect of subcarrier spacing (SCS) to the system performance has been determined by simulations. It has been observed that 50 Hz and 75 Hz SCSs result in a nearly identical performance and reducing SCS to 37.50 Hz does not improve the performance any further. Therefore, 50 Hz SCS is selected for further simulations. These results go hand in hand with DRM standard, where SCSs are selected to be from 47 to 107 Hz for robustness modes B to D, respectively, corresponding to parameterization for HF bands [4].

In the case of CP-OFDM and F-CP-OFDM, the length of CP is chosen to be 25 % (same as in DRM robustness mode B). For 50 Hz SCS this corresponds to CP duration of 5.00 ms. The roll-off factor for FMT is chosen to be $\alpha = 0.25$, in order to match the spectral efficiencies of FMT and CP-OFDM.

Fig. 4 illustrates the effect of CP length to BER performance of CP-OFDM in HF channel model E. As seen from this figure, CP length of 4.00 ms (20 %) would be sufficient since the RMS delay spread of HF channel model E is exactly 4.00 ms and the longest among the considered models. Fig. 5 illustrates the corresponding performance of FMT as a function of roll-off factor. It can be observed from this figure that the performance of FMT with roll-off of $\alpha = 1.0$ is approximately the same as for CP-OFDM with CP lengths of 20 % and 25 %, however, with reduced roll-off factor the performance gradually deteriorates. This is because the low-order time-domain equalizer used in the simulations is not able to equalize the considerably narrow transition-bands efficiently.

B. Frame and Pilot Structures

When designing the frame structure, some level of commonality with MIL-STD-188-110C [1] is also targeted. The proposed frame structure is based on long-term evolution (LTE)-like parameterization, where the subcarriers are scheduled into physical resource blocks (PRBs). Here, we have used PRB size of 16 subcarriers. The number of active carriers is chosen such

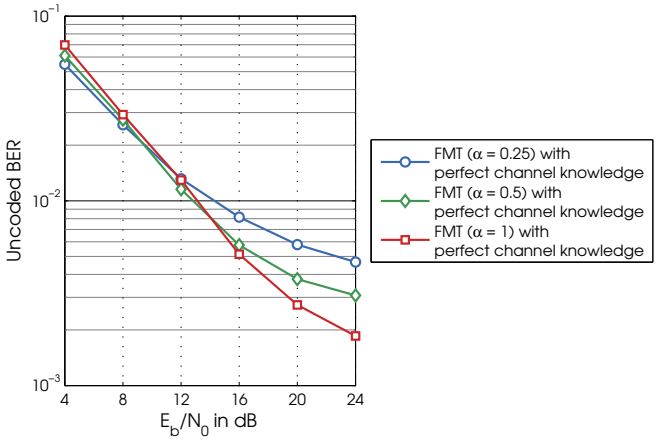

Fig. 5. Uncoded BER of FMT as a function of roll-off factor α in HF channel model E with perfect channel knowledge and QPSK modulation.

that the bandwidth of the signal is around 2400 Hz e.g., for 50 Hz SCS the number of active carriers is $M_{\text{act}} = 48$ requiring three PRBs.

The derivations in Section V and the preliminary studies clarified that the pilot density as high as 1/4 is required for the satisfactory performance for the most challenging channel model E. For this pilot pattern, the pilots are included in every subcarrier within each subframe as depicted in Fig. 1. The transmitted burst of data is composed of frames each consisting of four subframes. One subframe carries eight multicarrier symbols and, overall, one frame corresponds to the 1536 symbols (excluding the pilots).

C. Prototype Filter Design

The prototype filter design for F-CP-OFDM is carried out using techniques described in [12]. The transition-band width is selected to be equal to six times the subcarrier spacing. This selection gives fairly good performance as described in [12]. The FC block processing is carried out using overlap of 25 percent ($\lambda = 0.25$ in (3)). Fig. 6 shows the PSDs of

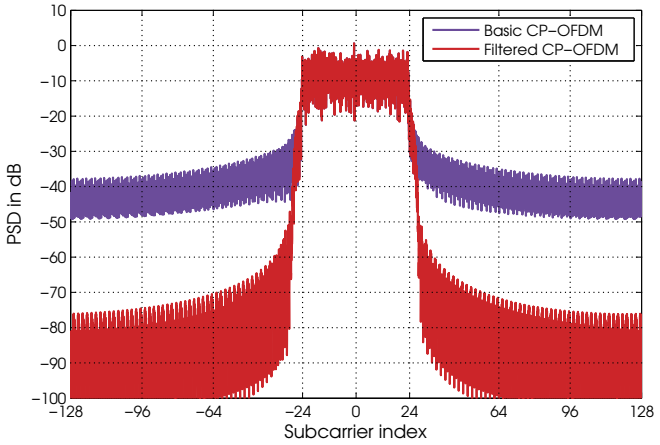

Fig. 6. Power spectral densities (PSDs) of the basic CP-OFDM and F-CP-OFDM.

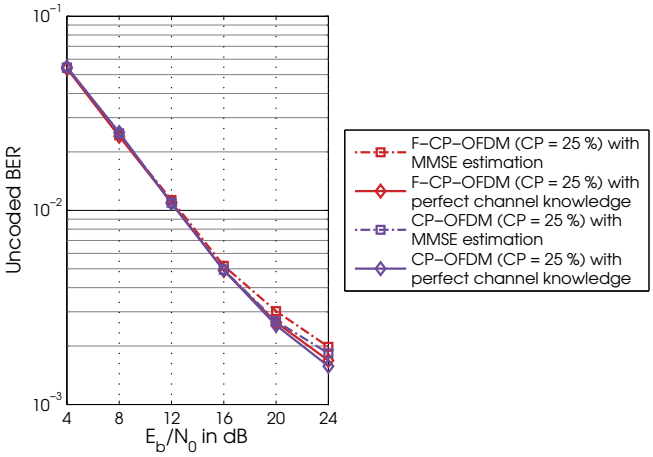

Fig. 7. Uncoded BER for CP-OFDM and F-CP-OFDM in HF channel model E. Perfect channel knowledge or MMSE estimation with exact pilots is used with QPSK modulation.

the basic CP-OFDM and F-CP-OFDM waveforms illustrating the considerably improved spectral containment of the latter waveform.

For FBMC/OQAM, the prototype filter design is based on the PHYDYAS polyphase prototype filter [29]. Here, we have used the overlapping factor of $K = 4$ and the design for which the total filter bank structure based self-interference is minimized.

The prototype filter for FMT is optimized by minimizing the stopband attenuation subject to constraint for the filter bank induced inter-symbol interference for a given overlapping factor K and roll-off factor α. In this case, considerably longer filter has to be used due to the smaller roll-off factor. The simulation results described later on are obtained using overlapping factor of $K = 12$.

VII. Numerical Results

A. Bit-Error Rate Performance

Fig. 7 shows the simulated uncoded BER of basic CP-OFDM and filtered CP-OFDM systems for HF channel model E and QPSK modulation. In this figure, results are shown both in the case of perfect channel knowledge and in the case when channel is known only at pilot positions. The pilot symbols are boosted on average by 2.50 dB with respect to data. The equalizer coefficients are updated for each symbol. For each simulation, 1000 burst transmissions with independent channel realizations are performed. As can be seen from this figure, the waveform filtering only slightly deteriorates the performance of F-CP-OFDM when compared with the basic CP-OFDM. This performance loss can be considered as negligible for feasible signal-to-noise ratio values.

Fig. 8 shows the simulated uncoded BER of FBMC/OQAM, FMT, and F-CP-OFDM in the case of perfect channel knowledge and the case when channel is assumed to be known at scattered pilot positions. For FBMC/OQAM, the equalizer coefficients are updated for each OQAM half-symbol whereas for FMT and F-CP-OFDM they are updated for each symbol. The combined pilot/auxiliary pilot symbol for FBMC/OQAM is boosted on average by 2.50 dB with respect to the data. The FMT and F-CP-OFDM pilots are boosted by the same value with respect to the data. As can be seen from these figures, F-CP-OFDM clearly outperforms FMT and FBMC/OQAM in the case of all channel models. It can also be observed that MMSE based channel interpolation is very close to perfect channel knowledge performance except for F-CP-OFDM and FMT there is a slight degradation in performance in the case of channel model F.

Fig. 10 shows the corresponding results in the case of perfect channel knowledge and the case when pilot based MMSE estimation employed. As seen from this figure, the performance loss when comparing the pilot-based estimation with the perfect channel knowledge is still tolerable for F-CP-OFDM and FMT, however, for FBMC/OQAM, considerably reduced performance is achieved. This performance loss is due to the fact that the auxiliary pilot-based scheme required by the FBMC/OQAM modulation is not able to provide good estimates in the case of fast-fading channel models and its performance is characterized by severe error floors at medium to high signal to noise ratios [30].

Overall, F-CP-OFDM seems to be the best alternative for HF communication with respect to its BER performance. However, in the case of coded system, the higher spectral efficiency of the FBMC/OQAM could be traded for increasing the coding gain and, therefore, further studies are needed to fairly compare these waveforms.

B. Computational Complexity

Table III gives the number real multiplications per complex symbol for all the considered schemes in the case when the number of subcarriers is $M = 256$. As seen from this table, the complexity of F-CP-OFDM and FMT are roughly four times that of the CP-OFDM whereas for FBMC/OQAM the complexity is only double. For conventional time-domain filter

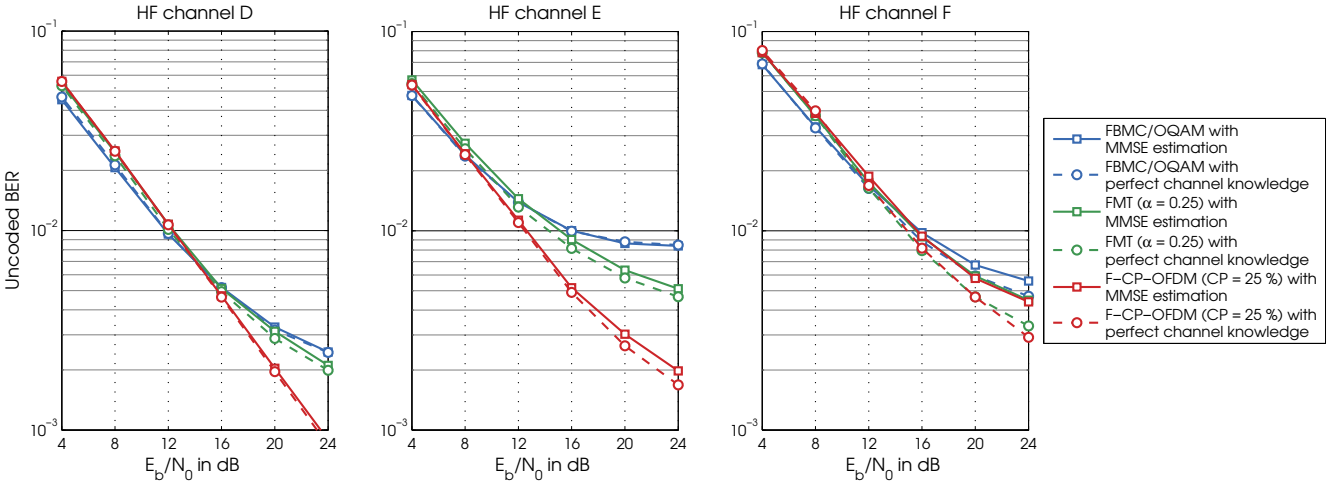

Fig. 8. Uncoded BER for filtered FBMC/OQAM, FMT, and CP-OFDM in HF channel models D, E, and F. Perfect channel knowledge or MMSE estimation using exact pilot values is used with QPSK modulation.

TABLE III
COMPLEXITY OF CONSIDERED MCM SCHEMES

MCM	Real multiplications	Relative complexity
CP-OFDM	37.58	1.00
F-OFDM	163.28	4.34
FBMC/OQAM	80.25	2.14
FMT	165.58	4.45

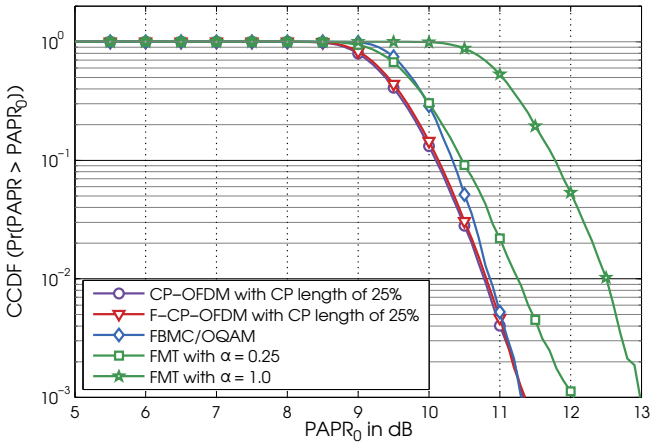

Fig. 9. The complementary cumulative distribution (CCDF) function for the considered MCM schemes.

realization, the impulse response length has to be 139 in order to meet the specification of FC-based filter. Therefore, the total number of real multiplications required for the OFDM processing and conventional filtering is 368.51 per complex symbol, which is more than double the complexity of FC-based implementation.

C. Peak-to-Average Power Ratio

The complementary cumulative distribution functions (CCDFs) of PAPR for all the multicarrier waveforms under consideration are illustrated in Fig. 9. In this figure, PAPR is evaluated over single frame. As seen from this figure, CCDF of F-CP-OFDM is the same as for basic CP-OFDM whereas for FBMC/OQAM a slight increase in PAPR is introduced. For FMT, the PAPR is reduced as the roll-off factor is reduced and for roll-off factor of $\alpha = 0.25$, the PAPR is approximately 0.50 dB larger than that of the CP-OFDM and F-CP-OFDM.

VIII. CONCLUDING REMARKS

We have compared the performance of three multicarrier modulation techniques with commonly adopted high-frequency channel models. It is shown that cyclic prefix orthogonal frequency-division multiplexing has clearly the best performance with doubly-dispersive channel models, also in the case when the waveform has been filtered for better spectral containment. The coded system performance remains as an important issue for further studies. In addition, the future work is devoted in comparing the performance of the studied multicarrier waveforms with the corresponding single-carrier waveforms.

ACKNOWLEDGEMENT

This work was supported by the Scientific Advisory Board for Defence (MATINE).

REFERENCES

[1] *Interoperability and Performance Standards for Data Modems*, US Department of Defense MIL-STD-188-110C, Sept. 2011.

[2] M. Manoufali, H. Alshaer, P. Y. Kong, and S. Jimaa, "Technologies and networks supporting maritime wireless mesh communications," in *Proc. Joint IFIP Wireless and Mobile Networking Conference (WMNC)*, Apr. 2013, pp. 1–8.

[3] N. M. Maslin, *HF Communications: A Systems Approach*. Taylor & Francis Ltd, 2005.

[4] *Digital Radio Mondiale (DRM); System Specification*, ETSI ES 201 980 V4.1.1, Jan. 2014. [Online]. Available: http://www.drm.org/wp-content/uploads/2014/01/DRM-System-Specification-ETSI-ES-201-980-V4.1.1-2014-01.pdf

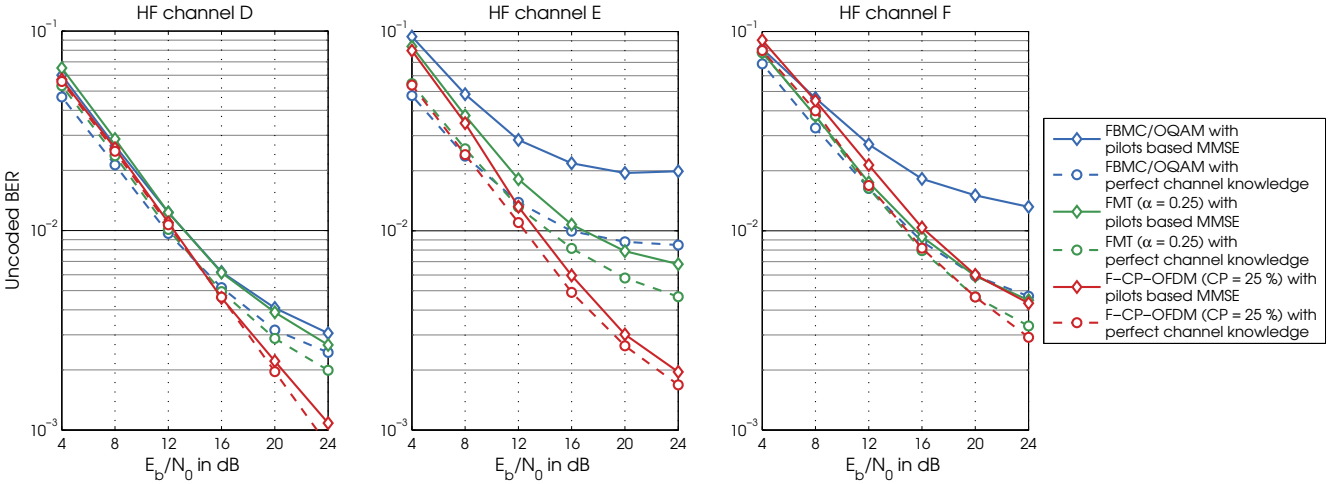

Fig. 10. Uncoded BER for filtered FBMC/OQAM, FMT, and CP-OFDM in HF channel models D, E, and F. Perfect channel knowledge or pilot based MMSE estimation is used with QPSK modulation.

[5] P. Siohan and M. Renfors, "Orthogonal communication waveforms," in *Orthogonal Waveforms and Filter Banks for Future Communication Systems*, M. Renfors, X. Mestre, E. Kofidis, and F. Bader, Eds. Elsevier/Academic Press, 2017, ch. 7, pp. 129–156.

[6] T. H. Stitz, T. Ihalainen, A. Viholainen, and M. Renfors, "Pilot-based synchronization and equalization in filter bank multicarrier communications," *EURASIP Journal on Advances in Signal Processing*, no. 2010:741429, 2010.

[7] P. Hoeher, S. Kaiser, and P. Robertson, "Two-dimensional pilot-symbol-aided channel estimation by Wiener filtering," in *Proc. Int. Conf. Acoust., Speech, Signal Processing (ICASSP)*, Ulm, Germany, June 29–July 4 1997, pp. 1845–1848.

[8] J. Yli-Kaakinen, M. Renfors, and H. Tuomivaara, "Multicarrier modulation for HF communications," in *Proc. Int. Conf. Military Commun. Information Syst. (ICMCIS)*, Brussels, Belgium, May 23–24 2016, pp. 1–7.

[9] A. Toskala and H. Holma, Eds., *LTE for UMTS – OFDMA and SC-FDMA Based Radio Access*. Wiley, 2009.

[10] M. Renfors, J. Yli-Kaakinen, T. Levanen, M. Valkama, T. Ihalainen, and J. Vihriälä, "Efficient fast-convolution implementation of filtered CP-OFDM waveform processing for 5G," in *2015 IEEE Globecom Workshops*, San Diego, CA, USA, Dec. 2015.

[11] M. AghababaeeTafreshi, J. Yli-Kaakinen, T. Levanen, V. Korhonen, P. Jääskeläinen, M. Renfors, M. Valkama, and J. Takala, "Parallel processing intensive digital front-end for IEEE 802.11ac receiver," in *Proc. Asilomar Conference on Signals, Systems, and Computers*, Nov. 8–11 2015.

[12] J. Yli-Kaakinen, T. Levanen, S. Valkonen, K. Pajukoski, J. Pirskanen, M. Renfors, and M. Valkama, "Efficient fast-convolution-based waveform processing for 5G physical layer," *IEEE Journal on Selected Areas in Communications*, vol. 35, no. 6, pp. 1309–1326, June 2017.

[13] P. Siohan, C. Siclet, and N. Lacaille, "Analysis and design of OFDM-OQAM systems based on filterbank theory," *IEEE Trans. Signal Processing*, vol. 50, no. 5, pp. 1170–1183, May 2002.

[14] B. Farhang-Boroujeny and R. Kempter, "Multicarrier communication techniques for spectrum sensing and communication in cognitive radios," *IEEE Communications Magazine, Special Issue on Cognitive Radios for Dynamic Spectrum Access*, vol. 46, no. 4, pp. 80–85, Apr. 2008.

[15] FP7-ICT Project PHYDYAS – Physical Layer for Dynamic Spectrum Access and Cognitive Radio. http://www.ict-phydyas.org.

[16] R. W. Chang, "Synthesis of band-limited orthogonal signals for multichannel data transmission," *The Bell System Technical Journal*, vol. 45, no. 10, pp. 1775–1796, Dec. 1966.

[17] G. Cherubini, E. Eleftheriou, and S. Ölçer, "Filtered multitone modulation for VDSL," in *Proc. of IEEE Global Telecommunications Conference (GLOBECOM)*, vol. 2, Rio de Janeireo, Brazil, 1999, pp. 1139–1144.

[18] N. Moret and A. M. Tonello, "Design of orthogonal filtered multitone modulation systems and comparison among efficient realizations," *EURASIP Journal on Advances in Signal Processing*, vol. 2010, no. 141865, 2014.

[19] I. Berenguer and I. J. Wassell, "FMT modulation: Receiver filter bank definition for the derivation of an efficient implementation," in *Proc. Int. OFDM Workshop*, Hamburg, Germany, Sept. 2002.

[20] K. Shao, L. Pi, J. Yli-Kaakinen, and M. Renfors, "Filtered multitone multicarrier modulation with partially overlapping sub-channels," in *Proc. Eur. Signal Process. Conf. (EUSIPCO)*, Kos island, Greece, Aug. 28–Sept.2 2017, pp. 425–429.

[21] W. Y. Zou and Y. Wu, "COFDM: An overview," *IEEE Transactions on Broadcasting*, vol. 41, no. 1, pp. 1–8, Mar. 1995.

[22] B. L. Floch, M. Alard, and C. Berrou, "Coded orthogonal frequency division multiplex," *Proc. IEEE*, vol. 5, no. 1, pp. 982–996, June 1995.

[23] H. V. Sorensen and C. S. Burrus, "Fast DFT and convolution algorithms," in *Handbook for Digital Signal Processing*, S. K. Mitra and J. F. Kaiser, Eds. New York: New York: John Wiley and Sons, Inc, 1993, ch. 8, pp. 491–610.

[24] J. Yli-Kaakinen, P. Siohan, and M. Renfors, "FBMC design and implementation," in *Orthogonal Waveforms and Filter Banks for Future Communication Systems*, M. Renfors, X. Mestre, E. Kofidis, and F. Bader, Eds. Elsevier/Academic Press, 2017, ch. 8, pp. 153–191.

[25] C. Watterson, J. Juroshek, and W. Bensema, "Experimental confirmation of an HF channel model," *IEEE Trans. Commun. Technol.*, vol. COM-18, no. 6, pp. 792–803, Dec. 1970.

[26] L. Vogler, J. Hoffmeyer, J. Lemmon, and M. Nesenbergs, "Progress and remaining issues in the development of a wideband HF channel model and simulator," in *Proc. Conf. Advisory Group for Aerospace Research and Development (AGARD): Propagation Effects and Circuit Performance of Modern Military Radio Systems with Particular Emphasis on Those Employing Bandspreading*, Paris, France, Oct. 1988.

[27] W. Xu, J. Berkmann, C. Carbonelli, C. Drewes, and A. Huebner, "Aspects of OFDM-based 3G LTE terminal implementation," in *Fourth-Generation Wireless Networks: Applications and Innovations*, S. Adibi, A. Mobasher, and T. Tofigh, Eds. IGI Global, 2010, pp. 526–564.

[28] T. Ihalainen, T. H. Stitz, M. Rinne, and M. Renfors, "Channel equalization in filter bank based multicarrier modulation for wireless communications," *EURASIP Journal on Advances in Signal Processing*, no. 2007:49389, 2007.

[29] A. Viholainen, M. Bellanger, and M. Huchard, "Prototype filter and structure optimization, ICT-211887 Project PHYDYAS (Physical Layer for Dynamic Access and Cognitive Radio) Technical Report D5.1," Jan. 2009. [Online]. Available: http://www.ict-phydyas.org/

[30] X. Mestre and E. Kofidis, "Pilot-based channel estimation for FBMC/OQAM systems under strong frequency selectivity," in *Int. Conf. Acoust., Speech, Signal Process. (ICASSP)*, Mar. 2016, pp. 3696–3700.